ELSEVIER

Neurobiology of Aging 33 (2012) 1651–1663

NEUROBIOLOGY OF AGING

www.elsevier.com/locate/neuaging

The noradrenaline precursor L-DOPS reduces pathology in a mouse model of Alzheimer's disease

Sergey Kalinin[a], Paul E. Polak[a], Shao Xia Lin[a], Amul J. Sakharkar[b,c], Subhash C. Pandey[b,c], Douglas L. Feinstein[a,c,*]

[a] *Department of Anesthesiology, University of Illinois at Chicago, Chicago, IL, USA*
[b] *Department of Psychiatry, University of Illinois at Chicago, Chicago, IL, USA*
[c] *Jesse Brown VA Medical Center, Chicago, IL, USA*

Received 28 December 2010; received in revised form 7 April 2011; accepted 29 April 2011

Abstract

Damage to noradrenergic neurons in the locus coeruleus (LC) is a hallmark of Alzheimer's disease (AD) and may contribute to disease progression. In 5xFAD transgenic mice, which accumulate amyloid burden at early ages, the LC undergoes stress as evidenced by increased astrocyte activation, neuronal hypertrophy, reduced levels of LC-enriched messenger RNAs (mRNAs), and increased inflammatory gene expression. Central nervous system (CNS) noradrenaline (NA) levels in 5-month-old male 5xFAD mice were increased using the NA precursor L-threo-3,4-dihydroxyphenylserine (L-DOPS). After 1 month, L-DOPS treatment improved learning in the Morris water maze test compared with vehicle-treated mice. L-DOPS increased CNS NA levels, and average latency times in the water maze test were inversely correlated to NA levels. L-DOPS reduced astrocyte activation and Thioflavin-S staining; increased mRNA levels of neprilysin and insulin degrading enzyme, and of several neurotrophins; and increased brain-derived neurotrophic factor protein levels. These data demonstrate the presence of LC stress in a robust mouse model of AD, and suggest that raising CNS NA levels could provide benefit in AD.

Keywords: Locus coeruleus; Noradrenaline; Tyrosine hydroxylase; GFAP; Morris water maze; Thioflavin-S; Droxidopa; Learning and memory; Neurotrophin; Neprilysin; Inflammation; Glial cells

1. Introduction

The primary source of noradrenaline (NA) in the central nervous system (CNS) derives from noradrenergic neurons present in the locus coeruleus (LC), located on the lateral face of the IV ventricle in the rostral pons. The LC has been characterized with respect to effects on arousal, stress, memory, and attention (Samuels and Szabadi, 2008; Sara, 2009); and with regulation of inflammation, neuronal survival, and neurogenesis (Marien et al., 2004). NA reduces inflammatory gene expression in glial cells and neurons (Benveniste et al., 1995; Feinstein et al., 1993; Madrigal et al., 2006; Szabó et al., 1997) and reduces neurotoxicity elicited by various stimuli including Aβ1–42 (Madrigal et al., 2007). In vivo, increasing NA using an α2-adrenergic receptor (AR) antagonist (Kalinin et al., 2006) or selective NA reuptake inhibitors (NARIs) reduced inflammatory gene expression (O'Sullivan et al., 2010); while treatment with a synthetic NA precursor provided benefit in mouse models of multiple sclerosis (Simonini et al., 2010) and Down's syndrome (Salehi et al., 2009).

These findings suggest that damage to LC neurons could have pathological consequences; a concept supported by findings that LC lesion exacerbates brain inflammation (Heneka et al., 2002; Pugh et al., 2007); and increases amyloid burden, neuronal damage, and behavioral deficits in transgenic mouse models of Alzheimer's disease (AD) ("TgAPP mice") (Heneka et al., 2006; Jardanhazi-Kurutz et al., 2010; Kalinin et al., 2007). In humans, LC cell numbers

* Corresponding author at: 835 South Wolcott Street, MC 513, Room E720, Chicago, IL 60612, USA. Tel.: +1 312 355 1665.
E-mail address: dlfeins@uic.edu (D. Feinstein).

0197-4580/$ – see front matter © 2012 Elsevier Inc. All rights reserved.
10.1016/j.neurobiolaging.2011.04.012

and brain NA levels are reduced during normal aging (Marien et al., 2004) and these losses are greater in AD (Adolfsson et al., 1979; German et al., 1992; Mann, 1983; Palmer and DeKosky, 1993; Weinshenker, 2008), and are correlated with plaque and tangle numbers (Bondareff et al., 1987) and duration of illness (Zarow et al., 2003). LC damage may therefore contribute to pathology occurring in AD.

LC damage also occurs in certain strains of TgAPP mice. Compared with controls, tyrosine hydroxylase (TH)-positive neurons in the LC were reduced in size in PDAPP mice (German et al., 2005), LC volume and neuronal cell numbers reduced in 8-month-old Tg2576 mice (Guérin et al., 2009), and the number of LC TH positive neurons were reduced in older PS: APP mice (Liu et al., 2008; O'Neil et al., 2007). NA levels were reduced in hippocampus (Szapacs et al., 2004) and cortex of older PS: APP mice (Pugh et al., 2007), and NA transporter messenger RNA (mRNA) levels lower in LC of PS: APP mice (Jardanhazi-Kurutz et al., 2010), consistent with LC damage. In the current study we confirm that LC damage and inflammation occur in 5xFAD TgAPP mice which develop amyloid plaque burden at an early age. Furthermore, treatment with an NA precursor reduced plaque burden, glial inflammation, and improved learning.

2. Methods

2.1. Materials

The racemic mixture DL-threo-3,4-dihydroxyphenylserine (DL-DOPS, catalog D2384) which contains 50% of the active form L-threo-3,4-dihydroxyphenylserine (L-DOPS), DL-serine 2-(2,3,4-trihydroxybenzyl) hydrazide hydrochloride (benserazide, catalog B7283), (R)-tomoxetine hydrochloride (atomoxetine, catalog T7947), and Thioflavin-S (TS, catalog T-1892) were from Sigma Chemical Co. (St. Louis, MO, USA). The Aβ1-42 ELISA kit (catalog KHB3544) was from BioSource Invitrogen (Carlsbad, CA, USA); the NA ELISA kit (catalog BA E-6200) was from Rocky Mountain Diagnostics Inc. (Colorado Springs, CO, USA).

2.2. Animals

In these studies we used 5xFAD mice (Oakley et al., 2006), which harbor 3 mutations in the amyloid precursor protein (APP) gene and 2 in the presenilin-1 (PS1) gene; they accumulate soluble Aβ1–42 and develop plaques by 4 to 5 weeks age, and show frank neuronal damage including intraneuronal accumulation of Aβ1–42 and cognitive deficits by age 5 months. Mice were generated by crossing male heterozygous 5xFAD mice to wild-type C57BL/6 female mice; followed by polymerase chain reaction (PCR) analysis for the presence of the APP transgene. After completion of treatments and behavior testing, the mice were anesthetized, sacrificed, 1 hemibrain fixed in paraformaldehyde (PFA) and frozen for immunohistochemistry, and the other half dissected, snap-frozen and kept at −80 °C for isolation of proteins and RNAs. All procedures used were approved by local Institution for Animal Care and Use Committees.

2.3. Treatments

Male 5xFAD mice and wild-type littermates aged 4.5 months were treated 3 times per week for 1 month with L-DOPS together with the L-aromatic amino acid decarboxylase (L-AAAD) inhibitor benserazide to reduce peripheral conversion, and the NA reuptake inhibitor (NARI) atomoxetine to increase extracellular NA levels. DL-DOPS was dissolved in 0.2 N HCl then neutralized with NaOH to reach a final concentration of 40 mg/mL. Benserazide was added to the neutralized DL-DOPS solution to give a final concentration of 12.5 mg/mL; and atomoxetine added to give a final concentration of 2 mg/mL. Mice (weighing approximately 20 g) received a 200 μL intraperitoneal injection to give a final dose of 400 mg/kg DL-DOPS which provides 200 mg/kg of the active L-DOPS enantiomer, 125 mg/kg benserazide, and 20 mg/kg atomoxetine. Controls received equivalent amounts of the vehicle.

2.4. Behavior testing

The Morris water maze test was performed as follows: water was poured into a round steel tank (150 cm diameter, 40 cm height), and a clear cylindrical platform (10 cm diameter, 30 cm height) was placed 1.0 cm below the water level in the middle of a fixed quadrant. The water temperature was adjusted to 21 °C. One day after the final administration of L-DOPS or vehicle, the memory trial test was performed twice, then 4 times daily for 2 days, and then twice on the fourth day for a total of 12 trials. The person doing the behavior testing was blinded to animal groups. A control group (n = 9) of age-matched male wild-type mice served as a positive control. Trials were always given 2 in a row per session, and mice were dried off between 2 trials. The mice were allowed to swim freely to seek the hidden platform and were left for an additional 20 seconds on the platform. Mice who did not find the platform within 60 seconds were placed onto the platform for 20 seconds; the latency time is defined as the time spent to reach the platform and remain on it for at least 3 seconds. The platform position was not moved during any of the trials. The start position was changed daily. The swimming path of each mouse was recorded by an overhead digital video camera and analyzed by a tracking system, EthoVision XT 6.0 (Noldus Information Technology, Wageningen, the Netherlands). The Morris water maze test was carried out twice using 2 different cohorts of 5xFAD male mice; the first had 13 mice per group (vehicle- and L-DOPS-treated); the second had 7 per group. The average latency times per trial were calculated from data derived from both studies (n = 20 per group). On the same day after the last trial, and 1 week later, mice were given a probe test in which the platform

was removed and time spent swimming in the target and opposite quadrants measured.

2.5. Measurements of noradrenaline levels

Cortical lysates were prepared by homogenization on ice of 1 mg wet weight tissue into 40 μL of 0.01 N HCl, 1 mM EDTA, and 4 mM sodium metabisulfite. NA levels in aliquots were determined by specific enzyme-linked immunosorbent assay (ELISA) according to manufacturer's instructions.

2.6. Measurements of Aβ1-42 levels

Aβ1–42 levels were measured by specific ELISA according to manufacturer's instructions. In brief, mouse hippocampal samples were dissected, snap-frozen on dry ice, homogenized in buffer (5 M guanidine HCl, 50 mM Tris-HCl, pH 8.0), incubated at room temperature for 3 hours and then serially diluted in the provided buffer containing protease inhibitor Cocktail Set III (Calbiochem Cat 539134, Merck, Darmstadt, Germany). The Aβ1–42 levels in samples were calculated by comparing to provided human Aβ1–42 standard, and normalized to hippocampal protein concentrations determined by Bradford assay (Bio-Rad, Hercules, CA, USA).

2.7. Immunohistochemistry

Hemibrains were fixed overnight in 4% paraformaldehyde in 0.1 M phosphate buffer, kept overnight in 10% sucrose in 0.1 M phosphate buffer, then frozen in isopentane at −30 °C. Serial sagittal sections (35 μM thick) were prepared on a cryostat, and stored in cryoprotective solution (0.1 M phosphate buffer:ethyleneglycol:glycerol 30:40:30) at −20 °C. The sections were cut between about 0.4 and 2.0 mm from midline which contains the entire LC (located between about 0.6 and 1.2 mm) as well as cells from the substantia nigra (SN) and ventral tegmental area (VTA). Sections were incubated overnight at 4 °C with primary antibody directed against glial fibrillary acidic protein (GFAP) using rat monoclonal anti-GFAP (2.2B10) [40] at dilution 1:500; or rabbit polyclonal anti-TH at 1:300 (Pel-Freeze, Rogers, AK, USA). After overnight incubation, sections were washed, incubated with fluorescently conjugated secondary antibodies, washed, cover slips applied, and slides kept at 4 °C until analysis.

For TS staining tissue sections were first mounted on glass slides, then incubated 5 minutes in 1% solution of TS in double-distilled H_2O, followed by two 5-minute washes in 80% vol/vol ethanol. The TS stained slides were allowed to air-dry and cover slipped using Vectashield mounting medium (Vector Laboratories catalog H-1000, Burlingame, CA, USA). Sections were viewed at 100× using a 10× objective, and the average plaque number and % area stained per section determined.

2.8. Image analysis

Images were obtained on a Zeiss Axioplan 2 microscope with an MRm AxioCam for image acquisition and densitometric analysis conducted using AxioVision version 4.0 software (Carl Zeiss, Inc, Thornwood, NY, USA). Image acquisition was conducted on sections stained simultaneously and exposed for identical amounts of time. One rectangular field of view (1050 μm × 1420 μm, total area 1.5 mm^2) taken at 100× magnification was analyzed per section. Quantitation of GFAP was done using an object area cut off of 10 μm^2 to include cell bodies and processes. The data were analyzed to determine the total number of positively stained objects per field of view, and the total area covered by positively stained objects presented as a percentage of the total field of view. Quantitation of TH-stained cell bodies was accomplished using an object area cut off of 60 μm^2 to exclude counting of processes. TH data were analyzed to determine the total number of positively stained cell bodies per field of view, and the average cell body size using the cell's long axis.

2.9. Gold immunolabeling for BDNF in cortex and hippocampus

Sagittal brain sections of 35-μm thickness were used for gold-immunolabeling for brain-derived neutrophic factor (BDNF) protein (Prakash et al., 2008). In brief, sections were washed in phosphate-buffered saline (PBS), followed by incubation in RPMI-1640 medium containing L-glutamine (Invitrogen, Grand Island, NY, USA) for 30 minutes. Sections were incubated in 10% normal goat serum diluted in PBS containing 0.25% Triton X-100 (PBST) for 30 minutes followed by incubation in 1% bovine serum albumin (BSA) (in PBST) for 30 minutes. Sections were incubated with antibody against BDNF (BDNF-H117; Santa Cruz Biotechnology, Santa Cruz, CA, USA), diluted (1:200) in 1% BSA, and prepared in PBST for 18 hours at room temperature. For negative control sections the primary antibody was omitted. Sections were washed in PBS (2 × 10 minutes), then in 1% BSA in PBS (2 × 10 minutes) followed by incubation in gold particle-conjugated anti-rabbit secondary antibodies (Nanoprobes, Inc., Yaphank, NY, USA) for 1 hour at room temperature. Sections were rinsed in 1% BSA in PBS followed by ddH_2O (3 × 3 minutes each) and gold particles were silver enhanced using silver Enhancement Kit (Ted Pella, Inc., Redding, CA, USA). Sections were washed in tap water, mounted, dehydrated through graded alcohols, cover-slipped using distyrene-plasticizer-xylene (DPX), and examined under a light microscope. Immunolabeled gold particles were counted at high magnification (100×) using the Image Analysis System (Loats Associates, Westminster, MD, USA). The threshold value was adjusted for each image such that the areas without staining gave 0 counts. Counting was performed for 3 areas each from 3 different sections (total 9

object fields) from each animal, and the values converted to number of immunogold particles in a 100-μm^2 area.

2.10. mRNA analysis

Total RNA was isolated using Trizol reagent (Invitrogen Gibco, Carlsbad, CA, USA). Cortical RNA was isolated from a section of cerebral cortex located immediately above the hippocampus. RNA from in and around the LC was isolated from a 1.5 × 1.5 mm sample dissected from the ventral lateral surface of the fourth ventricle, and extending from about −1.0 to −2.0 mm from the intra-aural line (Paxinos and Franklin, 2001). Quantitative PCR (qPCR) was carried out using TaqMan 384-well micro Fluidic cards (Applied Biosystems, Carlsbad, CA, USA) with primers designed to span an intron and amplify alternatively spliced transcripts. These included genes implicated in LC maturation, neuronal survival, adrenergic signaling, NA synthesis, and general inflammation (Table 1). The qPCR was carried out in a 7900 HT machine (Applied Biosystems), and analyzed using DataAssist V2.0. Calculated cycle take off (Ct) values were used to calculate relative mRNA levels normalized to values measured for α-actin in the same samples.

Table 1
Screening of cortical RNA samples for transcripts implicated in amyloid processing, neuronal survival and maturation, and adrenergic signaling

Gene	Ratio L-DOPS:vehicle	*p*-value	
Amyloid processing and clearance			
IDE	1.20	0.016	[a]
NEP	1.25	0.019	[a]
BACE2	1.19	0.063	ns
APP	1.11	0.327	ns
BACE1	1.11	0.495	ns
PSEN1	1.04	0.599	ns
PSEN2	1.05	0.623	ns
Neuronal growth and survival			
NGF	1.66	0.024	[a]
BDNF	1.55	0.028	[a]
Syn	1.21	0.006	[b]
NeuN	1.25	0.084	ns
NT-3	1.14	0.625	ns
TrkB	1.03	0.692	ns
TrkA	0.92	0.739	ns
NTN	0.99	0.917	ns
Adrenergic signaling and neuronal maturation			
DBH	1.84	0.005	[b]
α1-AR	1.22	0.036	[a]
CREB	1.17	0.058	ns
β1-AR	1.18	0.282	ns
TH	1.15	0.289	ns
MASH1	0.94	0.707	ns
β2-AR	0.98	0.931	ns
Phox2a	1.36	0.298	ns
EAR2	1.15	0.250	ns
β3-AR	0.50	0.021	[a]

Key: L-DOPS, L-threo-3,4-dihydroxyphenylserine; ns, not significant, L-DOPS versus vehicle.
[a] $p < 0.05$.
[b] $p < 0.01$.

2.11. Statistical analyses

Group comparisons were done by unpaired *t* tests; latency times were analyzed by 2-way parametric repeated measures analysis of variance (ANOVA) to detect effects between groups tested and between trials; and 1-way nonparametric repeated measures ANOVA (Friedman test) to detect effects within 1 group. Correlations between NA levels and average latency time were done by Spearman nonparametric correlational analyses. Two-tailed tests were used; and p values < 0.05 were considered statistically significant.

3. Results

3.1. LC neuronal stress and glial inflammation are present in 5xFAD mice

We first examined the LC and nearby regions for evidence of increased glial inflammation (Fig. 1). We observed an increase in overall GFAP staining in the 5xFAD mice versus wild-type littermates (Fig. 1A and B) with strong staining in the ventral-central portion of the LC, and in the dorsal portion of the subcoerulean (SCD) nucleus, and scattered staining located rostral to the LC. Quantitative image analysis confirmed a statistically significant increase in the number of GFAP positively-stained cells in the 5xFAD mice (Fig. 1E). In contrast to the LC, we did not observe any significant increase of GFAP staining in or around TH-positive stained dopaminergic neurons in either the SN or adjacent VTA of 5xFAD mice (Fig. 1C, D, and F). The increase in GFAP staining in the LC was not directly associated with the presence of dense amyloid plaques because the LC shows relatively sparse Thioflavin S staining compared with other regions (Fig. 2).

Immunostaining for TH positively-stained cells was carried out in the same sections as described above. Although there was no significant difference in the number of TH positively-stained neuronal cell bodies per field of view (Fig. 3A), the average cell body size (Fig. 3B) was significantly increased (approximately 20%) in the 5xFAD mice, suggestive of neuronal stress or damage. Similar measurements carried out in the SN and VTA did not show any significant alteration in either TH-positive cell numbers or cell body size.

Additional evidence for LC stress and inflammation was obtained by quantitative real time qPCR analysis of RNA isolated from the LC and surrounding area. Comparison of relative mRNA expression levels revealed significant reductions in the LC of 5xFAD mice for the LC-enriched enzymes dopamine beta hydroxylase (DBH) and TH, and significant increases in levels for several markers of inflammation and glial activation including GFAP, the microglial activation markers CD45 and CD11b, and the inflammatory

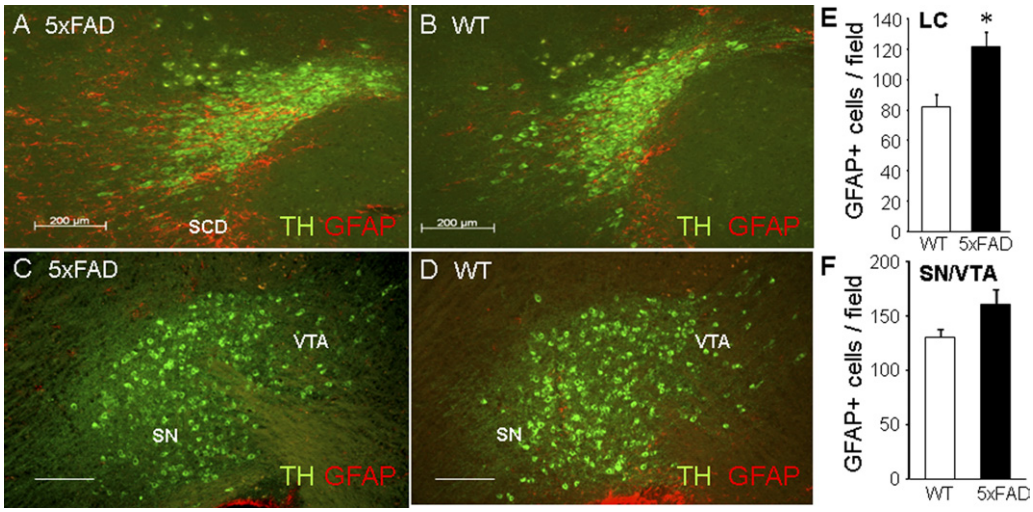

Fig. 1. Astrocyte activation is increased in the locus coeruleus (LC) of 5xFAD mice. Serial sagittal sections from 6-month-old male 5xFAD and wild-type age- and sex-matched littermates were stained with antibodies to tyrosine hydroxylase (TH; green) and glial fibrillary acidic protein (GFAP) (red). Representative sections show increased GFAP staining in and around the LC in (A) 5xFAD compared with (B) wild-type (WT) mice, but not around TH+ stained dopaminergic neurons in the substantia nigra (SN) or ventral tegmental area (VTA) (C and D). Quantitation of staining was done on 5 to 9 sections per mouse for the number of GFAP-positive stained objects (cell bodies and processes) in and around (E) the LC and (F) the SN and VTA present in the same and nearby sections. Data are mean ± standard error (SE) of number of objects per field of view, $n = 6$ or 7 mice per group. In panels (A) and (B) the fourth ventricle is located above and to the right. * $p < 0.05$ versus WT. SCD, dorsal subcoerulean nucleus. Scale bars are 200 μm.

proteins cyclooxygenase 2 (COX2) and nitric oxide synthase type 2 (NOS2) (Fig. 4).

3.2. Treatment with L-DOPS improves spatial learning

We tested the effects of treating 5xFAD mice with L-DOPS, a synthetic catecholamino acid which is converted to NA via decarboxylation by L-aromatic-amino-acid decarboxylase (L-AAAD) (Goldstein, 2006). Mice were treated with L-DOPS together with the L-AAAD inhibitor benserazide, which does not cross the blood-brain barrier, to reduce peripheral conversion of L-DOPS to NA and thereby increase the amount of L-DOPS that can enter the CNS, and with atomoxetine to selectively reduce NA reuptake. After 4-week treatment, cognitive testing using the Morris water maze was carried out (Fig. 5A). Two-way ANOVAs revealed significant differences by trial ($p < 0.0005$) and by group ($p < 0.05$); but a nonsignificant trial by group effect. In the individual groups, there was a significant decrease in latency time by trial in the L-DOPS-treated 5xFAD ($p = 0.019$) and the wild-type ($p = 0.041$) groups, but no improvement was observed in the vehicle-treated 5xFAD group (1-way ANOVA). Measurements of the distance swam to reach the platform (Fig. 5B) showed that in both wild-type (WT) and L-DOPS treated groups, but not the

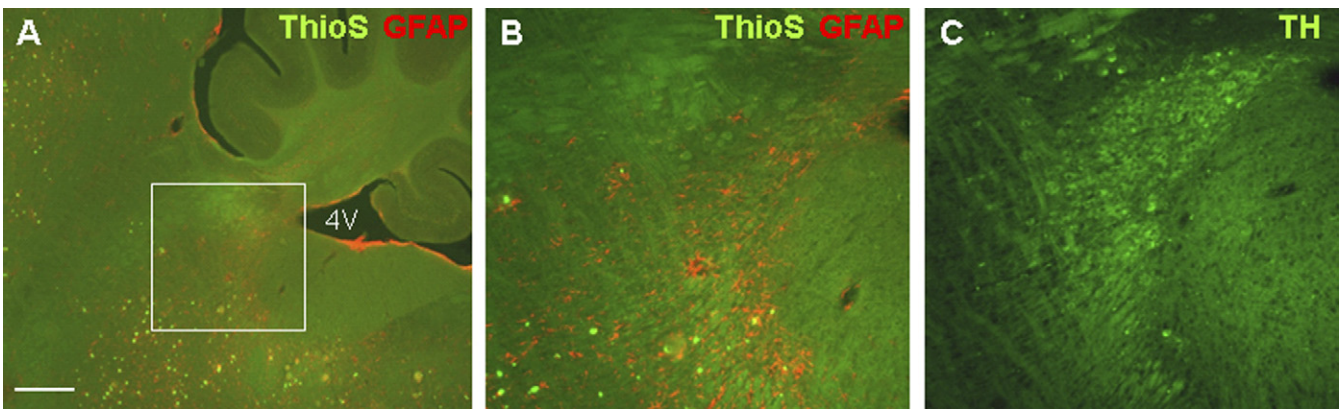

Fig. 2. Locus coeruleus (LC) glial activation is not closely associated with Thioflavin-S stained plaques. (A) Representative image from a sagittal section of 6-month-old male 5xFAD mouse stained with Thioflavin-S (green) and glial fibrillary acidic protein (GFAP) (red), illustrating absence of Thioflavin-S staining in the LC region (white box, magnified in panel B) and presence of GFAP positive staining. (C) A serial section from the same animal stained for tyrosine hydroxylase (TH; green) indicating the location of TH positively stained neurons in the LC. Scale bar is 500 μm.

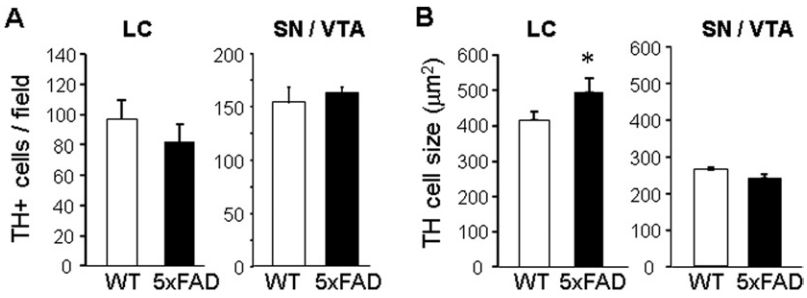

Fig. 3. Presence of tyrosine hydroxylase (TH)+ neuronal stress in the locus coeruleus (LC) of 5xFAD mice. The sections presented in Fig. 1 were quantified for (A) the number and (B) cell body size of TH-positively stained neurons in the LC and in the substantia nigra (SN) and ventral tegmental area (VTA). Data are mean ± standard error of 6 to 9 sections per mouse, 6 or 7 mice per group. * $p < 0.05$ versus wild-type (WT).

vehicle-treated group, there was a significant decrease over the 4-day training period, indicating that the faster latency times were not due to faster travel velocities. A probe test carried out after the last trial (Fig. 5C) showed that only the WT group spent significantly greater time in the target quadrant than the other quadrants. When a reprobe was done 1 week later none of the groups spent increased time in the target quadrant.

Analysis of lysates prepared from the above 5xFAD mice confirmed that treatment with L-DOPS significantly elevated NA levels in the frontal cortex (Fig. 5D). Interestingly, there was a significant inverse correlation between individual cortical NA levels and the latency time to find the platform averaged across all trials when data from both groups was combined, suggesting that higher NA levels are associated with improved learning (Fig. 5E).

3.3. Treatment with L-DOPS reduces glial activation and Aβ deposition

Treatment with L-DOPS reduced astroglial activation as assessed by staining for GFAP in both the cortex (Fig. 6A and B) and hippocampus (Fig. 6C and D). Quantitation showed a significant decrease in the total number of objects (cell bodies and processes) (Fig. 6E) and the % area stained (Fig. 6F) in both brain regions. Treatment with L-DOPS also reduced amyloid dense core plaque burden. Analysis of sagittal sections for Thioflavin S-stained plaques revealed modest (10%–20%) but significant reductions due to L-DOPS treatment in the number of plaques (Fig. 7A) and the % area covered (Fig. 7B) in both the hippocampus and the frontal cortex.

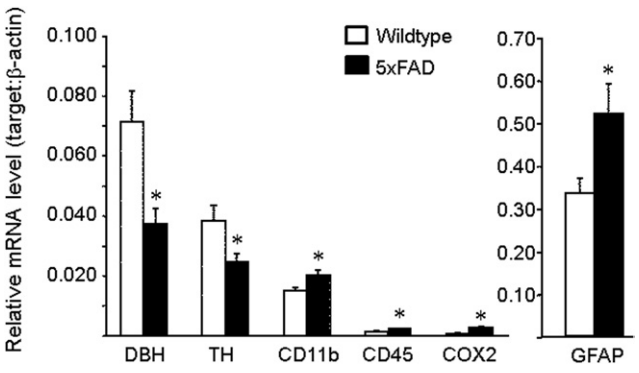

Fig. 4. Relative levels of catecholaminergic and inflammatory messenger RNAs (mRNAs) in the locus coeruleus (LC). RNA samples were prepared from the LC of 6-month-old male 5xFAD mice (filled boxes) and wild-type (WT; open boxes) male littermates ($n = 4$ per group), converted to complementary DNA (cDNA), and analyzed by real time quantitative polymerase chain reaction (qPCR). The data are mean ± standard error of the target mRNA level normalized to levels measured for β-actin in the same sample. * $p < 0.05$ versus WT.

To begin to determine how L-DOPS effects were being mediated, we screened cortical RNA samples for a panel of transcripts implicated in amyloid processing, neuronal survival, and adrenergic signaling and neuronal maturation (Table 1). Treatment with L-DOPS significantly increased levels of the amyloid-degrading enzymes NEP and IDE; of the neuronal marker synaptophysin 1, and the neurotrophins BDNF and nerve growth factor (NGF); and of the catecholaminergic marker DBH but not TH. Interestingly, L-DOPS increased expression of the α1-AR but decreased levels of the β3-AR. Cortical levels of the other measured mRNAs were not significantly different between L-DOPS and vehicle-treated samples; nor were any differences found in these markers in mRNA samples prepared from the hippocampus.

3.4. Treatment with L-DOPS increases BDNF protein expression

Because L-DOPS significantly increased mRNA levels for BDNF, a neurotrophic factor important for LC neuronal survival as well as being involved in processes of learning and memory, we tested the effects of L-DOPS on BDNF protein expression. Quantitative immunogold labeling of cortical (Fig. 8) and hippocampal (Fig. 9) sections revealed that L-DOPS significantly increased BDNF protein in these 2 regions.

4. Discussion

The current data demonstrate the presence of neuronal stress in the LC of relatively young (6-month-old) male

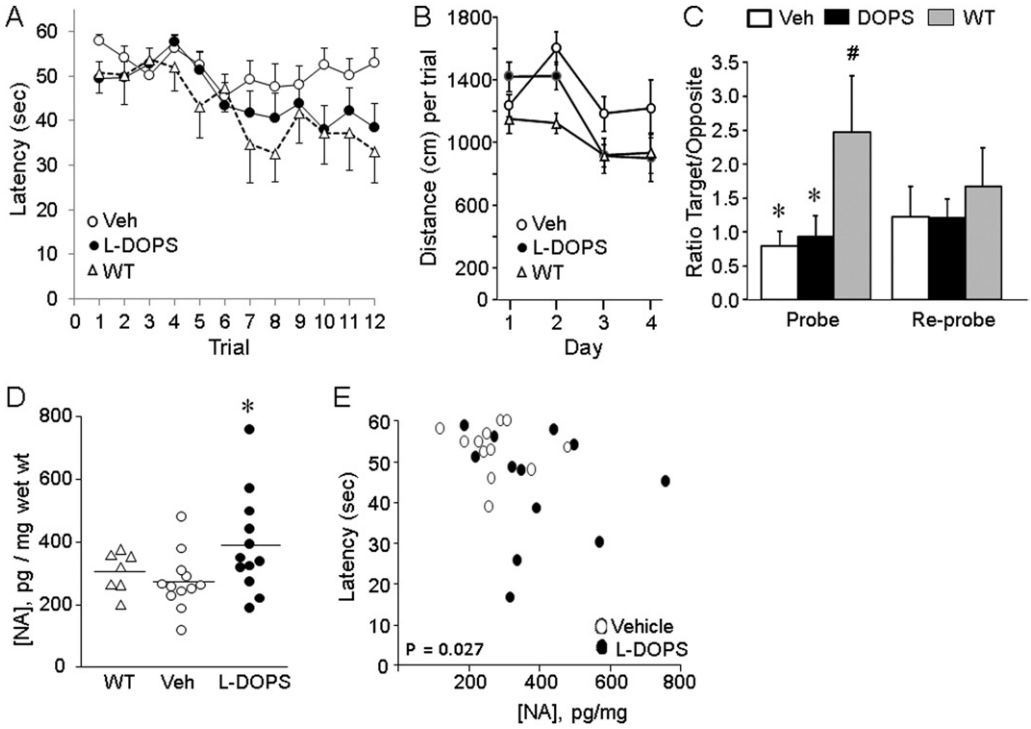

Fig. 5. L-threo-3,4-dihydroxyphenylserine (L-DOPS) improves learning in Morris water maze test. (A) Five-month old male 5xFAD mice were treated for 4 weeks (3 times per week) with vehicle (open circles) or L-DOPS (200 mg/kg) together with 125 mg/kg benserazide and 20 mg/kg atomoxetine (filled circles), after which behavioral training was done in the Morris water maze over 4 days. A group of 6-month-old male wild-type (WT) littermates (triangles) were also tested. Data are mean ± standard error ($n = 20$ mice per group for 5xFAD; $n = 9$ for WT) average latency time to find the hidden platform. For all 3 groups, there was a significant effect by trial ($p < 0.0005$) and by group ($p < 0.05$) but not a significant trial by group effect (2-way repeated measures analysis of variance [ANOVA]). Analysis of the individual group data showed a significant decrease by trial in L-DOPS-treated 5xFAD ($p = 0.019$) and WT groups ($p = 0.041$) but not in the vehicle-treated 5xFAD group (1-way repeated measures nonparametric ANOVA). (B) Measurements of the total distance swam show that for all 3 groups, there was a significant effect by trial ($p < 0.0005$) and by group ($p < 0.05$), and a significant trial by group effect ($p < 0.05$; 2-way repeated measures ANOVA). Analysis of the individual group data showed a significant decrease in distance swam by day for the L-DOPS-treated 5xFAD ($p < 0.005$) and WT ($p < 0.001$) groups, but not for the vehicle-treated group. Data are mean ± standard error of the mean distance swam averaged for each day of training. (C) In the probe test carried out immediately after training, only the WT mice spent a significantly greater percentage of time in the target quadrant relative to the opposite quadrant. In a reprobe test done 1 week later there was no preference shown by any group. * $p < 0.05$ versus WT, 1-way ANOVA Bonferroni post hoc; # $p < 0.05$ t test with hypothetical mean of 1.0 ratio time spent in target versus opposite quadrant. (D) Parenchymal noradrenaline (NA) levels were measured by specific enzyme-linked immunosorbent assay (ELISA) in lysates prepared from frontal cortices of 5xFAD mice after reprobe test. Data are mean ± standard error, $n = 13$ for vehicle and L-DOPS groups, $n = 7$ for WT group. * $p < 0.05$, 1-way ANOVA. (E) There was an inverse correlation ($p = 0.027$, Spearman analysis) between latency time averaged across all days versus cortical NA levels for data combined from all 5xFAD mice ($n = 26$ total); correlations for either group alone did not reach statistical significance.

5xFAD mice, as evidenced by hypertrophy of TH-positive neurons which was associated with increased astrocyte activation and inflammatory gene expression. We also measured reductions in expression of messenger RNAs (mRNAs) coding for TH and DBH, enzymes critical for NA synthesis. In view of these and other findings that suggest perturbations in LC function and NA levels occur in AD patients and transgenic mouse models, we tested if treatment with a NA precursor would provide benefit in 5xFAD mice. Although NARIs have been used to increase extracellular NA levels, their efficacy may be limited in the context of significant LC damage. In contrast, conversion of L-DOPS to NA should occur independent of LC pathology, and moreover because L-AAAD is expressed in both neurons and glial cells L-DOPS could exert beneficial effects on several cell types. Treatment of 5-month-old male 5xFAD mice for 1 month with L-DOPS increased CNS NA levels; significantly reduced staining for GFAP; reduced the number of Thioflavin-S-stained dense core plaques; and improved learning in the Morris water maze. Although we coadministered atomoxetine along with L-DOPS, the observed effects most likely require L-DOPS because when used alone atomoxetine did not show any significant effects on plaque burden in 5xFAD mice (SK, DLF, unpublished findings); the related NARI reboxetine did not improve behavior in PS: APP mice (personal communication, D. Weinshenker, March 2011); and atomoxetine did not improve cognitive deficits when tested in AD patients (Mohs et al., 2009); or clinical scores in a mouse model of multiple sclerosis (Simonini et al., 2010).

Interestingly, we found that GFAP staining was increased in the area of the LC, despite the absence of amyloid

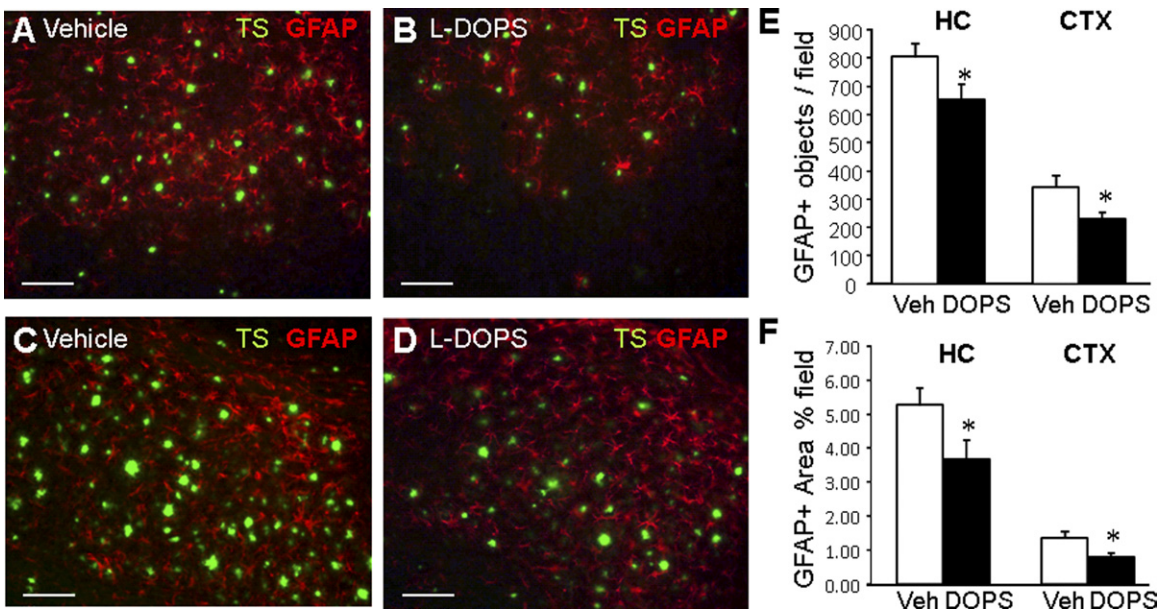

Fig. 6. Effects of L-threo-3,4-dihydroxyphenylserine (L-DOPS) on glial fibrillary acidic protein (GFAP) expression. Sagittal sections through (A and B) frontal cortex and (C and D) hippocampus of vehicle and L-DOPS-treated 5xFAD mice described in Fig. 5 were costained for GFAP (red) and Thioflavin-S (TS; green), then (E) the number of GFAP positively-stained objects per field of view (cell bodies and processes) and (F) the % area stained was quantified in 3 sections per mouse. Data are mean ± standard error; $n = 12$ or 13 mice per group. * $p < 0.05$ versus vehicle. Scale bar is 500 μm.

plaques as detected by TS staining. This could be due to the fact that TS stains dense core plaques; however studies using antibodies directed against Aβ1–42 or Aβ1–40 did not report strong staining in the cerebellum adjacent to the LC (Oakley et al., 2006). Whether increased astrocyte activation is due to the presence of soluble forms of amyloid beta, or an indirect consequence of increased LC neuronal stress is not known. However, LC damage leading to reductions in local levels of NA would be expected to be permissive for increased glial activation, and therefore treatment with L-DOPS could work in part by reducing glial activation in this region, as well as associated LC neuronal damage, as in the rest of the brain (as indicated in Table 1).

While we did not fully explore the basis for reduced plaque burden, our findings that L-DOPS increased the mRNA levels of 2 enzymes involved in amyloid clearance, neprilysin and IDE, suggest that increases in the activity of 1 or both of these enzymes could play a role. In a previous study, we showed that reduction of brain NA levels, using the LC-selective neurotoxin DSP4, led to an increase in amyloid burden which was directly correlated to reductions in neprilysin activity (Kalinin et al., 2007). It therefore is not unexpected that raising NA levels would lead to an increase in neprilysin expression. However, there is emerging data to support that NA increases the activity of resident glial cells to phagocytose amyloid (Heneka et al., 2010; Kalinin et al., 2006), and that loss of this activity in DSP4-treated TgAPP mice can be restored with L-DOPS (Heneka et al., 2010). Additionally, findings that inflammatory stimuli can increase the expression of amyloid processing enzymes such

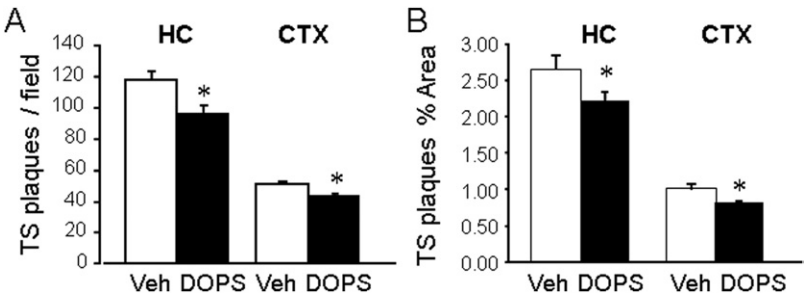

Fig. 7. Effects of L-threo-3,4-dihydroxyphenylserine (L-DOPS) on Thioflavin S (TS)-stained plaques. Thioflavin-S staining in the hippocampus and frontal cortex of vehicle and L-DOPS treated 5xFAD mice described in Fig. 5 was quantified from 3 sections per mouse for (A) the average number of TS stained plaques per field of view; and (B) the % field of view covered by plaques. The data are mean ± standard error; $n = 12$ or 13 mice per group and * $p < 0.05$ versus vehicle.

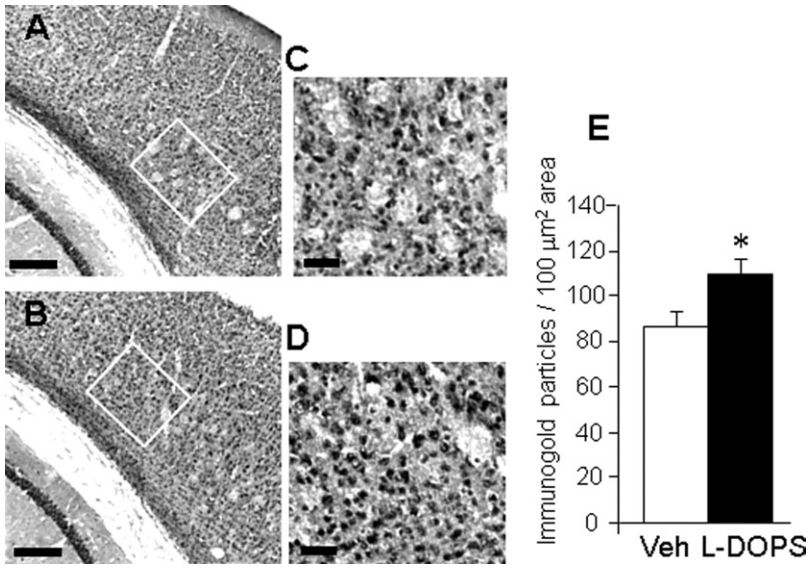

Fig. 8. L-threo-3,4-dihydroxyphenylserine (L-DOPS) increases cortical brain-derived neutrophic factor (BDNF) expression. Sagittal sections through the cortical brain region of (A and C) vehicle and (B and D) L-DOPS-treated 5xFAD mice described in Fig. 5 were stained by immunogold labeling (visible as small black particles) for the presence of BDNF protein. (E) The number of immunogold particles per 100 μm^2 was determined in 3 sections per animal. Data are mean ± standard error of $n = 6$ mice per group. * $p < 0.05$ versus vehicle. Boxes in panels (A) and (B) are magnified in panels (C) and (D). Scale bars, (A and B) 200 μm; (C and D) 50 μm.

as beta-1-secretase (Heneka and O'Banion, 2007; Sastre et al., 2008) suggests that the anti-inflammatory actions of elevated NA could lead to reduced amyloid production, as has been described for several other more commonly used nonsteroidal anti-inflammatory drugs (Cole and Frautschy, 2010; Szekely and Zandi, 2010).

Our observations of LC neuronal hypertrophy, in the absence of frank neuronal loss, are indicative of neuronal stress; which may account for decreased TH and DBH mRNA levels in the LC. The presence of neurons with swollen cell bodies has been described in both AD and Parkinson's disease brains (Chan-Palay, 1991), although cell atrophy (Mann, 1983) and selective loss of large neurons (Hoogendijk et al., 1995) was observed in some AD

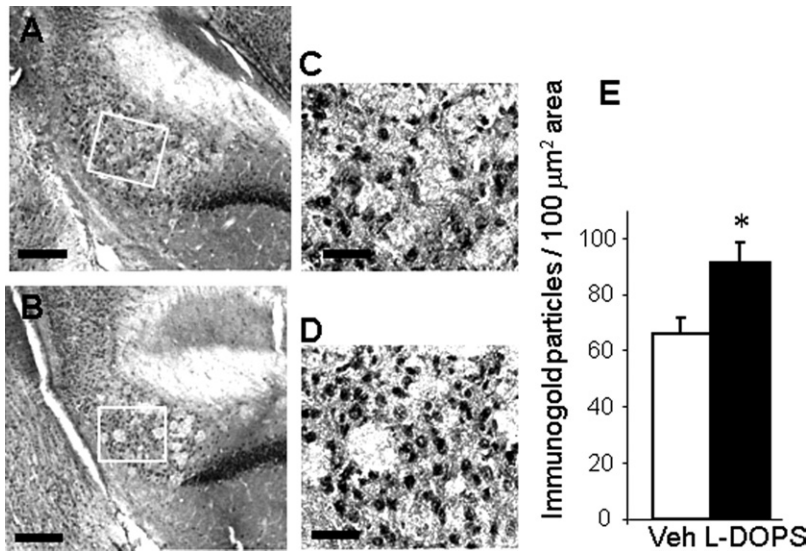

Fig. 9. L-threo-3,4-dihydroxyphenylserine (L-DOPS) increases hippocampal brain-derived neutrophic factor (BDNF) expression. Sagittal sections through the hippocampus of (A and C) vehicle- and (B and D) L-DOPS-treated 5xFAD mice described in Fig. 5 were stained by immunogold labeling (visible as small black particles) for the presence of BDNF protein. (E) The number of immunogold particles per 100 μm^2 in the subiculum was determined in 3 sections per animal. Data are mean ± standard error of $n = 6$ mice per group. * $p < 0.05$ versus vehicle. Boxes in (A) and (B) are magnified in (C) and (D). Scale bars, (A and B) 200 μm; (C and D) 50 μm.

patients. In contrast to our findings of neuronal hypertrophy, LC neuronal shrinkage was reported to occur in 24-month-old PDAPP mice (German et al., 2005). The smaller neurons were located to the dorsal-central region of the LC, while neurons in the rostral portion were of similar size to those in the wild-type littermates. Differences in the specific mouse strain (PDAPP versus 5xFAD) and ages (24 versus 6 months) may in part account for this, because neuronal hypertrophy may represent an earlier response during the progression of LC damage that ultimately leads to neuronal atrophy. Another difference is that in our studies the average LC cell size was calculated based on all TH positively-stained neurons identified; not only those present in the dorsal portion of the LC. In addition, our studies were carried out using sagittal sections and gave an average TH cell size of about 400 μm^2 in wild-type mice; analysis of the PDAPP mice were done using coronal sections and gave average cell sizes between 134 and 170 μm^2 in 24-month-old controls. Regardless of the precise explanation for these differences, the current data confirm the presence of endogenous LC neuronal stress and inflammation in a mouse model of AD occurring at a relatively young age. It should be mentioned that although damage to the LC clearly occurs in AD and some TgAPP strains, there is evidence for compensatory effects occurring including increased TH mRNA expression, sprouting of TH+ dendrites, and sprouting of TH+ axons (Szot et al., 2006, 2007) which could limit the therapeutic potential of treatments such as L-DOPS in older AD patients or at later stages of disease.

In this study we tested for possible benefits of L-DOPS on cognitive deficits by testing in the Morris water maze. In vehicle-treated 5xFAD mice, there was no improvement in the time to find the hidden platform after 12 trials, whereas a cohort of age- and sex-matched wild-type mice showed significant improvement over time. Poor learning in the Morris water maze has been previously reported for 5xFAD mice. In the original report, 4- to 6-month-old 5xFAD mice showed worse learning than wild-type littermates after 12 sessions of 2 trials each over 4 days (Ohno et al., 2006); while in a recent study 7- to 9-month-old female 5xFAD mice did not show any improvement after being trained 4 times per day for 9 days (Urano and Tohda, 2010). In contrast, we found that in the L-DOPS group a significant improvement occurred during training. Our findings that L-DOPS also reduced amyloid burden and inflammation in the hippocampus is consistent with the fact that learning in the Morris water maze test is considered to be dependent on hippocampal function (Tsien et al., 1996). Because NA is important for several forms of learning independently from its anti-inflammatory or neuroprotective actions, our findings may also be due in part to acute effects as observed in the mouse model of Down's syndrome (Salehi et al., 2009).

Interestingly, the mice with the shorter latency times (averaged across all 12 trials) had higher cortical NA levels. This correlation only reached significance when data from both the vehicle and the L-DOPS groups were combined; however, inspection of the data in Fig. 5D shows that some mice in the L-DOPS group had lower NA levels than the average in the vehicle group, suggesting that additional factors determine the efficacy of L-DOPS treatment, and improved methods (higher or more frequent dosing) may be needed to more reproducibly increase NA levels. It is also apparent that cortical NA levels measured at the end of the testing cannot be interpreted as a direct measure of pathology, because there were no significant differences measured between the wild-type and the vehicle-treated 5xFAD mice (Fig. 5D). Whether NA levels are different at this time in other brain regions, or whether the NA present is no longer sufficient to exert its anti-inflammatory or neuroprotective effects is not yet known.

Our results using L-DOPS can be compared with those recently reported on the effects of chronically increasing CNS NA levels in bigenic PS: APP mice using an alternative method, namely treatment with an α2-antagonist (Scullion et al., 2011). The mice used (TASTPM line) overexpress human APP with the Swedish mutation and PS1 with the M146V mutation, and normally develop pathology by age 5 to 6 months. The mice were administered the selective α2-antagonist fluparoxan (1 mg/kg per day, oral) continuously in the water beginning at age 4 months (before any pathology is evident). In contrast to our findings, treatment with fluparoxan had no significant effect on learning in the Morris water maze when tested after 4-month treatment, although it did provide significant improvement in the spontaneous alternation test. As found with L-DOPS, fluparoxan reduced astrocyte activation; in contrast they did not find any significant effect on amyloid burden assessed by immunostaining for plaques in either the cortex or hippocampus. This contrasts with the significant reductions due to L-DOPS in Thioflavin S-stained plaques we observed in both cortex and hippocampus. There are several possible reasons for this difference. Thioflavin S selectively stains dense core plaques, therefore increased NA may slow down the accumulation, or promote dis-aggregration, of dense core plaques with lesser effects on diffuse plaques. A second possibility is that a greater increase of NA in glial cells due to L-DOPS (which is converted to NA in glial cells as well as in neurons) compared with flupararoxan (primarily acting on neurons) could increase glial phagocytosis and clearance of amyloid. Differences between the mouse strains used (5xFAD vs. TASTPM) could also be an important factor, particularly because the 5xFAD mice accumulate soluble Aβ1–42 and develop plaques at very early ages, and also show intraneuronal accumulation of aggregated forms of Aβ1–42. The fact that L-DOPS reduced Thioflavin S stained plaques may help explain the discrepancy in Morris water maze results, because lower amyloid burden would be expected to reduce overall neuronal stress.

LC neuronal development and survival depends on various neurotrophins and their receptors (Arenas and Persson,

1994; Holm et al., 2003b), many of which are expressed in astrocytes and regulated by NA levels (Rémy et al., 2001); therefore changes in LC function or NA levels could influence glial expression of these factors. LC neurons normally express high levels of the BDNF receptor TrkB during development (Fawcett et al., 1998), and a critical role for BDNF in LC neuronal survival is suggested because TrkB deficient mice have 30% fewer LC neurons (Holm et al., 2003a), BDNF is a potent inducer of noradrenergic phenotype in primary LC cultures (Traver et al., 2006), and BDNF protects neurons against Aβ-induced cell death (Counts and Mufson, 2010). Our data show that mRNA as well as protein levels of BDNF are increased by L-DOPS, suggesting that increased BDNF in target regions of the LC could provide trophic support for LC neurons via retrograde transport mechanisms. In addition to its role as a survival factor, BDNF signaling is also involved in long-term potentiation (Minichiello, 2009) and BDNF levels are reduced in AD patients (Peng et al., 2005) and in TgAPP mice including 5xFAD (Kimura et al., 2010). Our results that L-DOPS increases hippocampal BDNF suggests that beneficial effects of NA on cognitive deficits may involve changes in this system.

Studies on the effects of L-DOPS in animal models of neurodegenerative diseases are limited. Two studies demonstrate a beneficial effect of L-DOPS when given acutely. In a mouse model of Down's syndrome, it was demonstrated that extensive LC degeneration occurs which is associated with deficits in contextual learning (Salehi et al., 2009). In those mice, acute treatment with L-DOPS (1000 mg/kg 1 time) led to significant improvement in learning measured 5 hours later (near the peak of increased hippocampal NA levels). In a recent AD-related study, the effects of L-DOPS on microglial functions in TgAPP mice was reported (Heneka et al., 2010). In that study, the LC was first lesioned using DSP4, which reduced microglial migration and phagocytosis of Aβ1–42. In the LC-lesioned mice, pretreatment with L-DOPS (administered at 1000 mg/kg 3 times over 24 hours) restored microglial migration and phagocytosis. Given the short duration of treatment, it is likely that the effects of increased NA in these 2 studies reflect changes in protein phosphorylation status due to rapid β-AR mediated increases in intracellular cyclic-AMP. In contrast, we showed using a mouse model of multiple sclerosis, that while L-DOPS rapidly (within days) prevented worsening of clinical signs, treatment with L-DOPS together with a NARI significantly reduced clinical scores only after about 3 weeks of treatment (Simonini et al., 2010).

L-DOPS is currently in phase III trials in the USA for treatment of neurogenic orthostatic hypotension, and is approved for such use in Asia. Therefore it may be reasonable to consider design of a pilot test of L-DOPS for AD patients; however there are several concerns that need to be kept in mind. A recent study in mild to moderately impaired AD patients using atomoxetine to raise CNS extracellular NA levels as an addition to ongoing cholinesterase-inhibitor therapy did not significantly improve cognitive function after 6 months (Mohs et al., 2009). However, while mean scores in the placebo group worsened over time, those in the treatment group did not, suggesting that atomoxetine delayed functional decline. The lack of benefit may be related to findings that increased NA significantly worsens agitation and anxiety in AD patients (Peskind et al., 2005). In this regard, treatment of patients with the selective α1-AR antagonist prazosin which blocks NA binding to α1-ARs improved symptoms of agitation and aggression (Wang et al., 2009), suggesting that treatment with L-DOPS together with an α1-antagonist may be clinically preferable. Finally, in view of accumulating evidence that LC damage plays a role in AD pathology, it is of interest to consider methods to selectively improve LC neuronal survival or activity, as is being considered for PD patients by targeting dopaminergic neuronal survival with virally-encoded growth factors (Rangasamy et al., 2010).

Disclosure statement

The authors declare that there are no actual or potential conflicts of interest.

All procedures used were approved by local Institution for Animal Care and Use Committees.

Acknowledgements

This work was supported in part by grants from the Department of Veterans Affairs, the American Alzheimer's Association, the NIH (RO1-AA010005 to SCP), and from Partnership for Cures (www.4cures.org). We thank Dr. Marc Marien for continued support, advice, and suggestions. Parts of this work were presented as a Webinar at the Alzheimer's Forum and can be viewed at www.alzforum.org/res/for/journal/detail.asp?liveID=186.

References

Adolfsson, R., Gottfries, C.G., Roos, B.E., Winblad, B., 1979. Changes in the brain catecholamines in patients with dementia of Alzheimer type. Br. J. Psychiatry 135, 216–223.

Arenas, E., Persson, H., 1994. Neurotrophin-3 prevents the death of adult central noradrenergic neurons in vivo. Nature 367, 368–371.

Benveniste, E.N., Huneycutt, B.S., Shrikant, P., Ballestas, M.E., 1995. Second messenger systems in the regulation of cytokines and adhesion molecules in the central nervous system. Brain Behav. Immun. 9, 304–314.

Bondareff, W., Mountjoy, C.Q., Roth, M., Rossor, M.N., Iversen, L.L., Reynolds, G.P., Hauser, D.L., 1987. Neuronal degeneration in locus ceruleus and cortical correlates of Alzheimer disease. Alzheimer Dis. Assoc. Disord. 1, 256–262.

Chan-Palay, V., 1991. Alterations in the locus coeruleus in dementias of Alzheimer's and Parkinson's disease. Prog. Brain Res. 88, 625–630.

Cole, G.M., Frautschy, S.A., 2010. Mechanisms of action of non-steroidal anti-inflammatory drugs for the prevention of Alzheimer's disease. CNS Neurol. Disord. Drug Targets 9, 140–148.

Counts, S.E., Mufson, E.J., 2010. Noradrenaline activation of neurotrophic pathways protects against neuronal amyloid toxicity. J. Neurochem. 113, 649–660.

Fawcett, J.P., Bamji, S.X., Causing, C.G., Aloyz, R., Ase, A.R., Reader, T.A., McLean, J.H., Miller, F.D., 1998. Functional evidence that BDNF is an anterograde neuronal trophic factor in the CNS. J. Neurosci. 18, 2808–2821.

Feinstein, D.L., Galea, E., Reis, D.J., 1993. Norepinephrine suppresses inducible nitric oxide synthase activity in rat astroglial cultures. J. Neurochem. 60, 1945–1948.

German, D.C., Manaye, K.F., White, C.L., III, Woodward, D.J., McIntire, D.D., Smith, W.K., Kalaria, R.N., Mann, D.M., 1992. Disease-specific patterns of locus coeruleus cell loss. Ann. Neurol. 32, 667–676.

German, D.C., Nelson, O., Liang, F., Liang, C.L., Games, D., 2005. The PDAPP mouse model of Alzheimer's disease: locus coeruleus neuronal shrinkage. J. Comp. Neurol. 492, 469–476.

Goldstein, D.S., 2006. L-Dihydroxyphenylserine (L-DOPS): a norepinephrine prodrug. Cardiovasc. Drug Rev. 24, 189–203.

Guérin, D., Sacquet, J., Mandairon, N., Jourdan, F., Didier, A., 2009. Early locus coeruleus degeneration and olfactory dysfunctions in Tg2576 mice. Neurobiol. Aging 30, 272–283.

Heneka, M.T., Galea, E., Gavriluyk, V., Dumitrescu-Ozimek, L., Daeschner, J., O'Banion, M.K., Weinberg, G., Klockgether, T., Feinstein, D.L., 2002. Noradrenergic depletion potentiates beta -amyloid-induced cortical inflammation: implications for Alzheimer's disease. J. Neurosci. 22, 2434–2442.

Heneka, M.T., Nadrigny, F., Regen, T., Martinez-Hernandez, A., Dumitrescu-Ozimek, L., Terwel, D., Jardanhazi-Kurutz, D., Walter, J., Kirchhoff, F., Hanisch, U.K., Kummer, M.P., 2010. Locus ceruleus controls Alzheimer's disease pathology by modulating microglial functions through norepinephrine. Proc. Natl. Acad. Sci. U. S. A. 107, 6058–6063.

Heneka, M.T., O'Banion, M.K., 2007. Inflammatory processes in Alzheimer's disease. J. Neuroimmunol. 184, 69–91.

Heneka, M.T., Ramanathan, M., Jacobs, A.H., Dumitrescu-Ozimek, L., Bilkei-Gorzo, A., Debeir, T., Sastre, M., Galldiks, N., Zimmer, A., Hoehn, M., Heiss, W.D., Klockgether, T., Staufenbiel, M., 2006. Locus ceruleus degeneration promotes Alzheimer pathogenesis in amyloid precursor protein 23 transgenic mice. J. Neurosci. 26, 1343–1354.

Holm, P.C., Rodriguez, F.J., Kresse, A., Canals, J.M., Silos-Santiago, I., Arenas, E., 2003a. Crucial role of TrkB ligands in the survival and phenotypic differentiation of developing locus coeruleus noradrenergic neurons. Development 130, 3535–3545.

Holm, P.C., Rodriguez, F.J., Kresse, A., Canals, J.M., Silos-Santiago, I., Arenas, E., 2003b. Crucial role of TrkB ligands in the survival and phenotypic differentiation of developing locus coeruleus noradrenergic neurons. Development 130, 3535–3545.

Hoogendijk, W.J., Pool, C.W., Troost, D., van Zwieten, E., Swaab, D.F., 1995. Image analyser-assisted morphometry of the locus coeruleus in Alzheimer's disease, Parkinson's disease and amyotrophic lateral sclerosis. Brain 118, 131–143.

Jardanhazi-Kurutz, D., Kummer, M.P., Terwel, D., Vogel, K., Dyrks, T., Thiele, A., Heneka, M.T., 2010. Induced LC degeneration in APP/PS1 transgenic mice accelerates early cerebral amyloidosis and cognitive deficits. Neurochem. Int. 57, 375–382.

Kalinin, S., Gavrilyuk, V., Polak, P.E., Vasser, R., Zhao, J., Heneka, M.T., Feinstein, D.L., 2007. Noradrenaline deficiency in brain increases beta-amyloid plaque burden in an animal model of Alzheimer's disease. Neurobiol. Aging 28, 1206–1214.

Kalinin, S., Polak, P.E., Madrigal, J.L., Gavrilyuk, V., Sharp, A., Chauhan, N., Marien, M., Colpaert, F., Feinstein, D.L., 2006. Beta-amyloid-dependent expression of NOS2 in neurons: prevention by an alpha2-adrenergic antagonist. Antioxid. Redox Signal. 8, 873–883.

Kimura, R., Devi, L., Ohno, M., 2010. Partial reduction of BACE1 improves synaptic plasticity, recent and remote memories in Alzheimer's disease transgenic mice. J. Neurochem. 113, 248–261.

Liu, Y., Yoo, M.J., Savonenko, A., Stirling, W., Price, D.L., Borchelt, D.R., Mamounas, L., Lyons, W.E., Blue, M.E., Lee, M.K., 2008. Amyloid pathology is associated with progressive monoaminergic neurodegeneration in a transgenic mouse model of Alzheimer's disease. J. Neurosci. 28, 13805–13814.

Madrigal, J.L., Kalinin, S., Richardson, J.C., Feinstein, D.L., 2007. Neuroprotective actions of noradrenaline: effects on glutathione synthesis and activation of peroxisome proliferator activated receptor delta. J. Neurochem. 103, 2092–2101.

Madrigal, J.L., Russo, C.D., Gavrilyuk, V., Feinstein, D.L., 2006. Effects of noradrenaline on neuronal NOS2 expression and viability. Antioxid. Redox Signal. 8, 885–892.

Mann, D.M., 1983. The locus coeruleus and its possible role in ageing and degenerative disease of the human central nervous system. Mech. Ageing Dev. 23, 73–94.

Marien, M.R., Colpaert, F.C., Rosenquist, A.C., 2004. Noradrenergic mechanisms in neurodegenerative diseases: a theory. Brain Res. Brain Res. Rev. 45, 38–78.

Minichiello, L., 2009. TrkB signalling pathways in LTP and learning. Nat. Rev. Neurosci. 10, 850–860.

Mohs, R.C., Shiovitz, T.M., Tariot, P.N., Porsteinsson, A.P., Baker, K.D., Feldman, P.D., 2009. Atomoxetine augmentation of cholinesterase inhibitor therapy in patients with Alzheimer disease: 6-month, randomized, double-blind, placebo-controlled, parallel-trial study. Am. J. Geriatr. Psychiatry 17, 752–759.

O'Neil, J.N., Mouton, P.R., Tizabi, Y., Ottinger, M.A., Lei, D.L., Ingram, D.K., Manaye, K.F., 2007. Catecholaminergic neuronal loss in locus coeruleus of aged female dtg APP/PS1 mice. J. Chem. Neuroanat. 34, 102–107.

O'Sullivan, J.B., Ryan, K.M., Harkin, A., Connor, T.J., 2010. Noradrenaline reuptake inhibitors inhibit expression of chemokines IP-10 and RANTES and cell adhesion molecules VCAM-1 and ICAM-1 in the CNS following a systemic inflammatory challenge. J. Neuroimmunol. 220, 34–42.

Oakley, H., Cole, S.L., Logan, S., Maus, E., Shao, P., Craft, J., Guillozet-Bongaarts, A., Ohno, M., Disterhoft, J., Van, E.L., Berry, R., Vassar, R., 2006. Intraneuronal beta-amyloid aggregates, neurodegeneration, and neuron loss in transgenic mice with five familial Alzheimer's disease mutations: potential factors in amyloid plaque formation. J. Neurosci. 26, 10129–10140.

Ohno, M., Chang, L., Tseng, W., Oakley, H., Citron, M., Klein, W.L., Vassar, R., Disterhoft, J.F., 2006. Temporal memory deficits in Alzheimer's mouse models: rescue by genetic deletion of BACE1. Eur. J. Neurosci. 23, 251–260.

Palmer, A.M., DeKosky, S.T., 1993. Monoamine neurons in aging and Alzheimer's disease. J. Neural Transm. Gen. Sect. 91, 135–159.

Paxinos, G., Franklin, K.B.J., 2001. The Mouse Brain in Stereotaxic Coordinates, second ed. Academic Press, San Diego.

Peng, S., Wuu, J., Mufson, E.J., Fahnestock, M., 2005. Precursor form of brain-derived neurotrophic factor and mature brain-derived neurotrophic factor are decreased in the pre-clinical stages of Alzheimer's disease. J. Neurochem. 93, 1412–1421.

Peskind, E.R., Tsuang, D.W., Bonner, L.T., Pascualy, M., Riekse, R.G., Snowden, M.B., Thomas, R., Raskind, M.A., 2005. Propranolol for disruptive behaviors in nursing home residents with probable or possible Alzheimer disease: a placebo-controlled study. Alzheimer Dis. Assoc. Disord. 19, 23–28.

Prakash, A., Zhang, H., Pandey, S.C., 2008. Innate differences in the expression of brain-derived neurotrophic factor in the regions within the extended amygdala between alcohol preferring and nonpreferring rats. Alcohol. Clin. Exp. Res. 32, 909–920.

Pugh, P.L., Vidgeon-Hart, M.P., Ashmeade, T., Culbert, A.A., Seymour, Z., Perren, M.J., Joyce, F., Bate, S.T., Babin, A., Virley, D.J., Rich-

ardson, J.C., Upton, N., Sunter, D., 2007. Repeated administration of the noradrenergic neurotoxin N-(2-chloroethyl)-N-ethyl-2-bromobenzylamine (DSP-4) modulates neuroinflammation and amyloid plaque load in mice bearing amyloid precursor protein and presenilin-1 mutant transgenes. J. Neuroinflammation 4, 8.

Rangasamy, S.B., Soderstrom, K., Bakay, R.A., Kordower, J.H., 2010. Neurotrophic factor therapy for Parkinson's disease. Prog. Brain Res. 184, 237–264.

Rémy, S., Naveilhan, P., Brachet, P., Neveu, I., 2001. Differential regulation of GDNF, neurturin, and their receptors in primary cultures of rat glial cells. J. Neurosci. Res. 64, 242–251.

Salehi, A., Faizi, M., Colas, D., Valletta, J., Laguna, J., Takimoto-Kimura, R., Kleschevnikov, A., Wagner, S.L., Aisen, P., Shamloo, M., Mobley, W.C., 2009. Restoration of norepinephrine-modulated contextual memory in a mouse model of Down syndrome. Sci. Transl. Med. 1, 7ra17.

Samuels, E.R., Szabadi, E., 2008. Functional neuroanatomy of the noradrenergic locus coeruleus: its roles in the regulation of arousal and autonomic function part II: physiological and pharmacological manipulations and pathological alterations of locus coeruleus activity in humans. Curr. Neuropharmacol. 6, 254–285.

Sara, S.J., 2009. The locus coeruleus and noradrenergic modulation of cognition. Nat. Rev. Neurosci. 10, 211–223.

Sastre, M., Walter, J., Gentleman, S.M., 2008. Interactions between APP secretases and inflammatory mediators. J. Neuroinflammation 5, 25.

Scullion, G.A., Kendall, D.A., Marsden, C.A., Sunter, D., Pardon, M.C., 2011. Chronic treatment with the α(2)-adrenoceptor antagonist fluparoxan prevents age-related deficits in spatial working memory in APP×PS1 transgenic mice without altering β-amyloid plaque load or astrocytosis. Neuropharmacology 60, 223–234.

Simonini, M.V., Polak, P.E., Sharp, A., McGuire, S., Galea, E., Feinstein, D.L., 2010. Increasing CNS noradrenaline reduces EAE severity. J. Neuroimmune. Pharmacol. 5, 252–259.

Szabó, C., Haskó, G., Zingarelli, B., Németh, Z.H., Salzman, A.L., Kvetan, V., Pastores, S.M., Vizi, E.S., 1997. Isoproterenol regulates tumour necrosis factor, interleukin-10, interleukin-6 and nitric oxide production and protects against the development of vascular hyporeactivity in endotoxaemia. Immunology 90, 95–100.

Szapacs, M.E., Numis, A.L., Andrews, A.M., 2004. Late onset loss of hippocampal 5-HT and NE is accompanied by increases in BDNF protein expression in mice co-expressing mutant APP and PS1. Neurobiol. Dis. 16, 572–580.

Szekely, C.A., Zandi, P.P., 2010. Non-steroidal anti-inflammatory drugs and Alzheimer's disease: the epidemiological evidence. CNS Neurol. Disord. Drug Targets 9, 132–139.

Szot, P., White, S.S., Greenup, J.L., Leverenz, J.B., Peskind, E.R., Raskind, M.A., 2006. Compensatory changes in the noradrenergic nervous system in the locus ceruleus and hippocampus of postmortem subjects with Alzheimer's disease and dementia with Lewy bodies. J. Neurosci. 26, 467–478.

Szot, P., White, S.S., Greenup, J.L., Leverenz, J.B., Peskind, E.R., Raskind, M.A., 2007. Changes in adrenoreceptors in the prefrontal cortex of subjects with dementia: evidence of compensatory changes. Neuroscience 146, 471–480.

Traver, S., Marien, M., Martin, E., Hirsch, E.C., Michel, P.P., 2006. The phenotypic differentiation of locus ceruleus noradrenergic neurons mediated by brain-derived neurotrophic factor is enhanced by corticotropin releasing factor through the activation of a cAMP-dependent signaling pathway. Mol. Pharmacol. 70, 30–40.

Tsien, J.Z., Huerta, P.T., Tonegawa, S., 1996. The essential role of hippocampal CA1 NMDA receptor-dependent synaptic plasticity in spatial memory. Cell 87, 1327–1338.

Urano, T., Tohda, C., 2010. Icariin improves memory impairment in Alzheimer's disease model mice (5xFAD) and attenuates amyloid β-induced neurite atrophy. Phytother. Res. 24, 1658–1663.

Wang, L.Y., Shofer, J.B., Rohde, K., Hart, K.L., Hoff, D.J., McFall, Y.H., Raskind, M.A., Peskind, E.R., 2009. Prazosin for the treatment of behavioral symptoms in patients with Alzheimer disease with agitation and aggression. Am. J. Geriatr. Psychiatry 17, 744–751.

Weinshenker, D., 2008. Functional consequences of locus coeruleus degeneration in Alzheimer's disease. Curr. Alzheimer Res. 5, 342–345.

Zarow, C., Lyness, S.A., Mortimer, J.A., Chui, H.C., 2003. Neuronal loss is greater in the locus coeruleus than nucleus basalis and substantia nigra in Alzheimer and Parkinson diseases. Arch. Neurol. 60, 337–341.